

# Enthalpy Recovery of Glassy Polymers: Dramatic Deviations from the Extrapolated Liquidlike Behavior

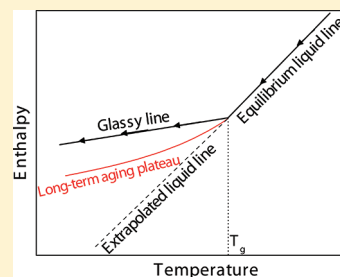
Virginie M. Boucher,<sup>†</sup> Daniele Cangialosi,<sup>\*,‡</sup> Angel Alegría,<sup>‡,§</sup> and Juan Colmenero<sup>†,‡,§</sup>

<sup>†</sup>Donostia International Physics Center, Paseo Manuel de Lardizabal 4, 20018 San Sebastián, Spain

<sup>‡</sup>Centro de Física de Materiales (CSIC-UPV/EHU), Paseo Manuel de Lardizabal 5, 20018 San Sebastián, Spain

<sup>§</sup>Departamento de Física de Materiales, Universidad del País Vasco (UPV/EHU), Apartado 1072, 20080 San Sebastián, Spain

**ABSTRACT:** We performed a systematic study on the recoverable enthalpy in several glass-forming polymers. We found that after prolonged isothermal physical aging the enthalpy reaches a plateau with values substantially larger than those corresponding to the enthalpy state extrapolated from the melt state. Enthalpy recovery experiments after up-jumps indicate that the enthalpy state corresponding to the plateau found after simple down-jump experiments is restored after long-term aging. This result is interpreted considering the plateau in the enthalpy as a thermodynamically stable state. We argue on the possible scenarios emerging from this conclusion. In particular, we discuss whether polymer glasses in the achieved thermodynamic state are stable over any time scale, or rather this corresponds to a relative minimum with further evolution at much larger time scales. Finally, the shift factor obtained from aging time–temperature superposition of enthalpy recovery data was found to considerably deviate from the Vogel–Fulcher–Tammann equation, normally adequate to describe the segmental mobility above the glass transition temperature ( $T_g$ ). The deviation of thermodynamics and dynamics from the behavior expected extrapolating the behavior from above  $T_g$  has been analyzed within the Adam–Gibbs framework, which actually relates the relaxation time and a thermodynamic magnitude, namely the configurational entropy. It has been found that, at least semiquantitatively for most of the investigated polymers, the connection between dynamics and thermodynamics holds also below  $T_g$ .



## INTRODUCTION

The normal fate of a liquid cooled down below its melting temperature is the achievement of the thermodynamically stable crystalline state. However, for kinetic reasons, crystallization can in many instances be avoided and a metastable liquid can exist even below the melting temperature.<sup>1</sup> Further temperature reduction eventually leads to the formation of a glass, namely a system with the mechanical properties of a solid but displaying no long-range atomic or molecular order. The crossover from the melt to the glassy state is commonly addressed as the glass transition. This phenomenon is kinetic in nature as the associated temperature—the glass transition temperature  $T_g$ —depends on the applied cooling rate. Given the ability of a large number of materials to form a glass, the physics of glass-forming liquids has been widely investigated in the past decades. In particular, both dynamic and thermodynamic aspects of glass-forming liquids—together with the associated glass transition—have been the subject of intense debate. Among them, polymers have been widely studied due to their good ability to form glasses. Nowadays, the achievement of a large number of experimental results has generally clarified these aspects above the  $T_g$  of the glass former, i.e., for relaxation times of the order of or smaller than seconds. Conversely, much less is known about the fate of the dynamics and the thermodynamics of glass-forming liquids below the so-defined  $T_g$ . This is especially relevant in polymer glasses due to the use of these systems in many applications in the glassy state.<sup>2</sup> Furthermore, this issue is of particular interest since

the extrapolation of available data obtained above  $T_g$  to lower temperatures generally produces a singularity in both dynamics and thermodynamics. In particular, the relaxation time associated with the glass transition is predicted to diverge at a finite temperature if empirical laws such as the Vogel–Fulcher–Tammann (VFT)<sup>3–5</sup> (or the Williams–Landel–Ferry equation (WLF))<sup>6</sup> are assumed to be valid also below  $T_g$ . The extrapolation of first-order thermodynamic variables also results in a singularity at a finite temperature, namely the temperature at which the thermodynamic properties of the glass would equal those of the crystal.<sup>7</sup> This would lead to the conclusion, against the third principle of thermodynamics, that below this temperature an amorphous system possesses a smaller entropy than the crystal counterpart. With some exceptions<sup>8,9</sup> the temperatures for dynamic (the Vogel temperature  $T_0$ ) and thermodynamic (the Kauzmann temperature  $T_K$ ) singularity are generally found to be approximately equal.<sup>10</sup>

In recent years, several theoretical<sup>11–15</sup> and experimental<sup>16–22</sup> works have been devoted to the study of the dynamics below  $T_g$  of glass-forming systems, including polymers. In all cases significant deviations from the VFT behavior toward a milder temperature dependence have been encountered. From the point of view of thermodynamics, several studies, both

**Received:** August 9, 2011

**Revised:** September 7, 2011

**Published:** September 21, 2011

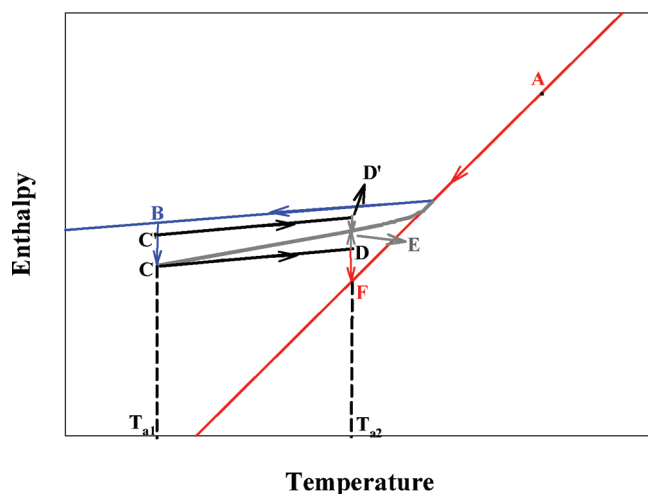


**Figure 1.** Schematic illustration of the temperature dependence of the enthalpy in the melt (red) and glassy (blue) state. The gray line represents the enthalpy corresponding to the plateau found after prolonged aging.

theoretical,<sup>23,24</sup> molecular dynamics simulation,<sup>25–27</sup> and experimental,<sup>28–33</sup> also seem to indicate deviations from the mere extrapolation of thermodynamic variables from above  $T_g$ , though—in comparison to those in the dynamics—these are seen at temperatures somewhat lower if  $T_g$  is taken as a reference.<sup>34,35</sup> In all cases the predicted or observed deviations are always in the direction of a decrease in the equilibrium specific heat. This implies that below  $T_g$  first-order thermodynamic variables decrease with temperature less rapidly than expected from mere extrapolation. This may possibly avoid the violation of the third law of thermodynamics.<sup>36</sup> Among the mentioned studies, a number of them<sup>28–33</sup> were based on monitoring enthalpy relaxation during prolonged aging below  $T_g$ . In all cases the recovered enthalpy appears to reach a plateau with no apparent evolution of the thermodynamic state during time. Interestingly, such a plateau corresponds to an enthalpy level considerably higher than that obtained extrapolating this magnitude from above  $T_g$ . Despite the appearance of this plateau, it is not yet clear whether this corresponds to an effective energy minimum or this plateau is only apparent and further reduction in enthalpy would occur at significantly longer times. Furthermore, recent results on vapor deposited low molecular weight glasses showed enthalpies considerably lower than those achieved after long-term aging.<sup>37,38</sup>

In the present work, we attempt to clarify the nature of the observed plateau in the enthalpy after prolonged physical aging in polymer systems. To do so, we first perform systematic long-term enthalpy recovery experiments in a wide temperature range below  $T_g$  on several glassy polymers, namely polystyrene (PS) with two different molecular weights, poly(methyl methacrylate) (PMMA), and polycarbonate (PC). These experiments aimed to characterize the line in the enthalpy versus temperature plot defining the plateau in the time evolution of the thermodynamic state of the glassy polymer. Having achieved this information, polymers were subjected to the following thermal cycle, schematized in Figure 1: (i) they were first aged at a temperature  $T_{a1}$  significantly smaller than  $T_g$ , in particular small enough to reach a plateau in the enthalpy consistently different from the extrapolated one; (ii) samples were subsequently heated up at a

temperature  $T_{a2}$  and the isothermal evolution of the enthalpy monitored. If the two aging temperatures,  $T_{a1}$  and  $T_{a2}$ , are adequately selected, the initial enthalpy at step (ii) will be intermediate between the extrapolated one and that corresponding to the plateau (for details see Experimental Section). Thus, the direction of enthalpy evolution (upward or downward) delivers information on the thermodynamically stable state of the glassy polymer. Further experiments after partial equilibration at an aging temperature  $T_{a1}$  and up-jump to  $T_{a2}$  followed by monitoring of the enthalpy recovery were performed to provide additional evidence on the independence of the achieved thermodynamic state from the thermal history. Furthermore, aging time—temperature superposition of enthalpy recovery data close to the plateau was performed. The temperature dependence of the so-obtained shift factor delivered information on the dynamics below  $T_g$ . Considering that both the shift factor and the enthalpy deviate from the behavior expected by simple extrapolation of data from above  $T_g$ , these two aspects were related to each other through the Adam–Gibbs (AG) approach.<sup>39</sup> This actually provides a connection between the dynamics and the thermodynamics of glass-forming polymers.<sup>8</sup>

## EXPERIMENTAL SECTION

Polystyrene (PS) and poly(methyl methacrylate) (PMMA) were purchased from Polymer Source Inc. and polycarbonate (PC) from Sigma-Aldrich. PMMA and PC respectively displayed the following molecular weights and distributions:  $M_w = 308\,000\text{ g mol}^{-1}$  and  $M_w/M_n = 1.5$ ;  $M_w = 34\,600\text{ g mol}^{-1}$  and  $M_w/M_n = 1.5$ . Two different PS were employed possessing the following molecular weights and distributions:  $M_w = 85\,000\text{ g mol}^{-1}$  and  $M_w/M_n = 1.02$  (labeled as PS85K);  $M_w = 7000\text{ g mol}^{-1}$  and  $M_w/M_n = 1.03$  (labeled as PS7K). The calorimetric  $T_g$  corresponding to a cooling rate of  $20\text{ K min}^{-1}$  are reported in Table 1.

Thermal analyses of the samples were carried out by means of a differential scanning calorimeter (DSC-Q2000) from TA Instruments. The temperature was calibrated with melting indium. All DSC measurements were performed under nitrogen atmosphere on samples of about 5 mg, placed in aluminum pans. All enthalpy recovery experiments began with a heating ramp to a temperature equal to or larger than  $T_g + 30\text{ K}$ , kept for 5 min, to erase the material's previous thermal history. For enthalpy recovery after down-jump from above  $T_g$  to the selected aging temperature  $T_a$ , samples were subsequently cooled down at  $20\text{ K min}^{-1}$  at a temperature considerably lower than  $T_a$  followed by stabilization at  $T_a$  and aged in the calorimeter for times from several minutes to 48 h before being cooled down to  $293\text{ K}$ , at a cooling rate of  $20\text{ K min}^{-1}$ , prior to reheating at  $10\text{ K min}^{-1}$  for data collection. For the measurements of the enthalpy relaxation at longer aging times ( $t_a > 48\text{ h}$ ), the annealing of the samples was carried out in an external vacuum oven, at  $T_a$ , after erasing of the thermal history and quenching of the samples in the DSC. After aging, the samples were quenched again and DSC thermograms recorded. Second scans were run immediately after a new cooling at  $20\text{ K min}^{-1}$ . The complete thermal procedure applied to the samples for the structural recovery study has been schematized in a previous work.<sup>32</sup>

Enthalpy recovery within the so-called “asymmetry of approach”<sup>46</sup> was conducted through the procedure exemplified in Figure 1: (i) samples were first cooled down at  $20\text{ K min}^{-1}$  to a temperature considerably lower than  $T_g$  and stabilized at  $T_{a1}$  and allowed to age until no time evolution in the enthalpy is detected (thermodynamic path A–B–C in Figure 1); (ii) samples were brought from  $T_{a1}$  to  $T_{a2}$  (C–D in Figure 1) and the enthalpy evolution was monitored with time.  $T_{a1}$  and  $T_{a2}$  were selected in such a way that the thermal cycle drawn in Figure 1 is respected. In particular, the main requirement of this procedure is that the initial enthalpy state at  $T_{a2}$  after prolonged aging at  $T_{a1}$  lays between the plateau line and the one extrapolated from the

**Table 1. Summary of All Parameters of the Investigated Glass-Formers<sup>a</sup>**

| polymer | $T_g$ (K) | $a$ (J g <sup>-1</sup> K <sup>-1</sup> ) | $b$ (J g <sup>-1</sup> K <sup>-1</sup> ) | $T_a$ (K)            | $\Delta H_{Tot}$ (J g <sup>-1</sup> ) | $\Delta H_{Extr}$ (J g <sup>-1</sup> ) | log $A$ (s) | $\beta_{KWW}$ | $x^b$ | $\Delta h^*/k$ (K) |
|---------|-----------|--|--|----------------------|---------------------------------------|--|-------------|---------------|-------|--------------------|
| PS7K    | 363       | 0.87                                     | −0.0015                                  | 359                  | 1.3                                   | 1.3                                    | −87.6       | 0.4           | 0.19  | 76 500             |
|         |           |  |  | 356                  | 1.75                                  | 2.3                                    | −86.9       | 0.35          | 0.15  |                    |
|         |           |  |  | 353                  | 2.34                                  | 3.3                                    | −86         | 0.3           | 0.1   |                    |
|         |           |  |  | 343                  | 2.94                                  | 6.8                                    | −87.3       | 0.3           | 0.1   |                    |
|         |           |  |  | 343–353 <sup>c</sup> | −0.6                                  |  | −86         | 0.3           | 0.1   |                    |
| PS85K   | 375       | 0.87                                     | −0.0015                                  | 369                  | 1.9                                   | 2.2                                    | −76         | 0.4           | 0.19  | 69 800             |
|         |           |  |  | 366                  | 1.96                                  | 3.1                                    | −76.4       | 0.4           | 0.19  |                    |
|         |           |  |  | 362                  | 2.2                                   | 4.4                                    | −76.7       | 0.4           | 0.19  |                    |
|         |           |  |  | 358                  | 2.27                                  | 5.75                                   | −77.3       | 0.4           | 0.19  |                    |
|         |           |  |  | 353                  | 2.34                                  | 7.4                                    | −77         | 0.35          | 0.15  |                    |
|         |           |  |  | 343                  | 2.41                                  | 10.9                                   | −78.9       | 0.35          | 0.15  |                    |
|         |           |  |  | 353–366 <sup>c</sup> | −0.55                                 |  | −76.4       | 0.4           | 0.19  |                    |
| PC      | 419       | 0.52                                     | −0.0006                                  | 414                  | 1.4                                   | 1.5                                    | −123.5      | 0.35          | 0.15  | 124 000            |
|         |           |  |  | 411                  | 1.7                                   | 2.4                                    | −122.7      | 0.3           | 0.1   |                    |
|         |           |  |  | 408                  | 2                                     | 3.3                                    | −123        | 0.3           | 0.1   |                    |
|         |           |  |  | 398                  | 2.2                                   | 6.4                                    | −125.4      | 0.3           | 0.1   |                    |
|         |           |  |  | 398–411 <sup>c</sup> | −0.65                                 |  | −122.7      | 0.3           | 0.1   |                    |
| PMMA    | 396       | 0.75                                     | −0.001                                   | 393                  | 0.67                                  | 1.05                                   | −56.6       | 0.5           | 0.29  | 54 500             |
|         |           |  |  | 388                  | 1.06                                  | 2.85                                   | −56.5       | 0.45          | 0.24  |                    |
|         |           |  |  | 383                  | 1.15                                  | 4.7                                    | −56.6       | 0.45          | 0.24  |                    |
|         |           |  |  | 378                  | 1.2                                   | 6.55                                   | −56.8       | 0.45          | 0.24  |                    |
|         |           |  |  | 368                  | 1.6                                   | 10.3                                   | −57.6       | 0.45          | 0.24  |                    |
|         |           |  |  | 353                  | 2.15                                  | 16.2                                   | −59.6       | 0.45          | 0.24  |                    |
|         |           |  |  | 353–378 <sup>c</sup> | −0.95                                 |  | −56.8       | 0.45          | 0.24  |                    |

<sup>a</sup>  $T_g$  and  $\Delta H_{Tot}$  (J g<sup>-1</sup>) are obtained from experiments.  $\Delta h^*$  is evaluated from literature data.<sup>18,40–43</sup> The parameter  $a$  and  $b$  to calculate  $\Delta C_p = a + bT$  are obtained from literature data.<sup>44,45</sup> Log  $A$ ,  $\beta_{KWW}$ , and  $x$  are obtained fitting enthalpy recovery curves to the TNM model (see text for details).

<sup>b</sup> Nonlinearity parameter related to the stretching exponent by  $x = (\beta_{KWW} - 0.2)/1.05$ . <sup>c</sup> Indicates up-jump to the higher temperature after equilibrating at the lower temperature.

melt state. This thermal cycle allows investigating the direction of the enthalpy evolution at  $T_{a2}$ : either from D to E or from D to F in Figure 1.

Further enthalpy recovery experiments were conducted by partially aging at  $T_{a1}$  for a time significantly smaller than that required to reach the plateau (path B–C' in Figure 1), then performing an up-jump to  $T_{a2}$  (path C'–D' in Figure 1), and finally allowing the thermodynamic state of the system to evolve.

As a general rule, in all the previously described thermal procedures, the amount of recovered enthalpy of a glass for a period of time  $t_a$  at a given temperature  $T_a$  was evaluated by integration of the difference between thermograms of aged and unaged samples, according to the relation<sup>47</sup>

$$\Delta H(T_a, t_a) = \int_{T_x}^{T_y} (C_p^a(T) - C_p^u(T)) dT \quad (1)$$

where  $C_p^a(T)$  and  $C_p^u(T)$  are respectively the specific heat of the aged and unaged samples and  $T_x$  and  $T_y$  are respectively temperatures (appropriately chosen) below and above the calorimetric  $T_g$ .

Apart from calorimetric data, we have employed literature data from broadband dielectric spectroscopy (BDS)<sup>18,40–42</sup>—providing information on the segmental dynamics above  $T_g$ —for the same polymers investigated in this study.

## RESULTS

Figure 2 (filled symbols) displays the temperature dependence of the specific heat at different aging times after a down-jump from above  $T_g$  with 20 K min<sup>-1</sup> cooling rate. Experiments

performed at one aging temperature for each polymer (indicated in the figure caption) are reported as a showcase. The main signature of enthalpy relaxation during physical aging is the development of an endothermic overshoot in the temperature range of the glass to liquid transition. This overshoot systematically shifts to higher temperatures and increases in magnitude with increasing aging time. Such behavior generally indicates increase of the recovered enthalpy during the course of physical aging. It is worth noticing that, among the investigated polymers, PMMA displays a peculiar evolution with the aging time of the specific heat versus temperature. In this case, differently from all other investigated polymers a prepeak appears and increases in magnitude with increasing aging time. This characteristic is specific of PMMA, at least among the polymers investigated in the present work, and has been already evidenced in the past.<sup>31,32,48,49</sup>

The time evolution of the recovered enthalpy—displayed as the difference between the total recoverable enthalpy (the very long time limit) and that recovered at each aging time—is displayed in Figure 3 for all investigated polymers and temperatures. The insets of Figure 3 show the temperature dependence of the total recovered enthalpy together with the enthalpy that would be recovered if the enthalpy of the melt was linearly extrapolated below  $T_g$ . The latter can be approximately obtained from  $\Delta H_{extr} = \Delta C_p(T_g - T)$ , where  $\Delta C_p$  is the difference between the melt and glass specific heats evaluated at  $T_g$ . This can be appropriately described by a linear function of the temperature:  $\Delta C_p = a + bT$ ,<sup>50</sup> where  $a$  and  $b$  are material specific

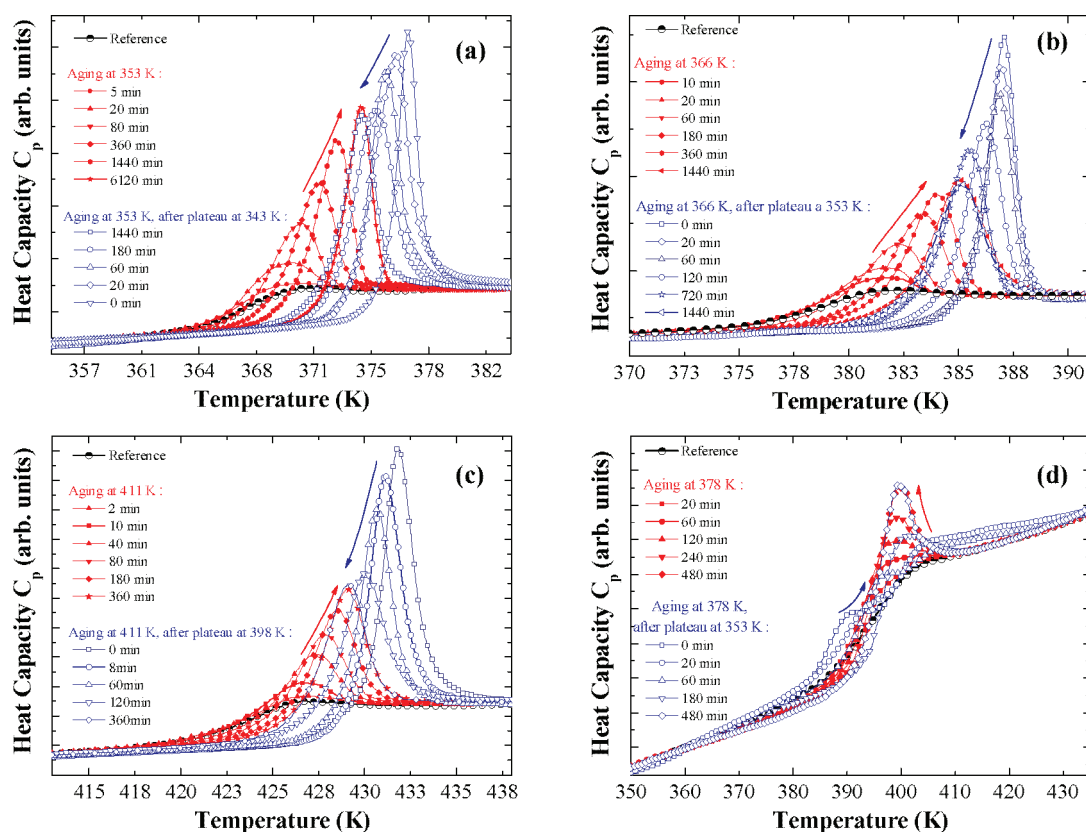


**Figure 2.** Specific heat versus temperature for different thermal histories, including down-jump (red filled symbols) and up-jump experiments (blue empty symbols), as obtained by DSC for (a) PS7K, (b) PS85K, (c) PC, and (d) PMMA. Details on the thermal history corresponding to the DSC scans are reported in the figure.

parameters reported in Table 1 determined fitting the obtained  $C_p$  versus temperature data. The  $\Delta C_p(s)$  obtained from our data generally agree with those available in the literature for the investigated polymers.<sup>44,45</sup> In the same table we report the total recovered enthalpy and the one that would be recovered in case the trend of the enthalpy above  $T_g$  was followed also at lower temperatures. From the observation of Figure 3, the following qualitative considerations can be made: (i) the total recoverable enthalpy increases with decreasing temperature; (ii) the time evolution of the recovered enthalpy appears to be highly stretched, covering several orders of magnitude in time; (iii) for the lowest investigated temperatures only a relatively small fraction of the extrapolated recoverable enthalpy is actually recovered; (iv) even for the lowest investigated temperatures lower than  $T_g$  by as much as about 40 K, the enthalpy reaches a plateau after aging times shorter than  $10^7$  s. The latter result is rather remarkable considering that the relaxation time of the  $\alpha$  process is generally expected to reach practically unfeasible time scales already at  $T_g - 10$  K.<sup>3–5</sup> This issue will be discussed in details in the Discussion section.

The inability of the enthalpy to evolve toward the extrapolated equilibrium is certainly an important outcome of the systematic study of the present work and agrees with a number of recent studies.<sup>28–33</sup> To get further insight on the nature of the observed plateau in the time evolution of the enthalpy, we have followed the evolution of the enthalpy after the thermodynamic path schematized in Figure 1: A–B–C–D. It is interesting to check whether the enthalpy of the glass—having a thermodynamic

state defined by point D at the aging temperature  $T_{a2}$ —evolves toward the previously defined plateau (point E in Figure 1) or toward the thermodynamic equilibrium (point F in Figure 1). This is shown in Figure 2 (open symbols) where the specific heat versus temperature is shown for different aging times starting from the thermodynamic state defined by point D in Figure 1. As is possible to observe in all cases the endothermic overshoot slowly evolves toward the specific heat versus temperature plot corresponding to the enthalpy state of the plateau obtained from standard down-jump experiments. Figure 4 displays the enthalpy evolution after the up-jump. In all cases the qualitative conclusion drawn from the observation of Figure 3, namely, that the enthalpy reaches the same value as that corresponding to the down-jump from above  $T_g$  to  $T_{a2}$  after prolonged aging, is quantitatively confirmed. This result implies that the plateau in the enthalpy observed after prolonged aging can be considered as a thermodynamically stable state rather than being kinetic in nature.

The latter observation is further corroborated by enthalpy recovery results at  $T_{a2}$  obtained after a third thermodynamic path, namely that indicated in Figure 1 as A–B–C'–D'. The specific heat versus temperature plot after prolonged aging at  $T_{a2}$  starting from D' is displayed in Figure 5 for PC as a showcase (similar results are obtained for the other polymers). In the same figure the specific heat versus temperature curve corresponding to the achievement of the plateau after simple down-jump to  $T_{a2}$  is shown. Figure 5 indicates that, whatever the thermal history of the glass—direct down-jump to  $T_{a2}$  or first partial annealing at



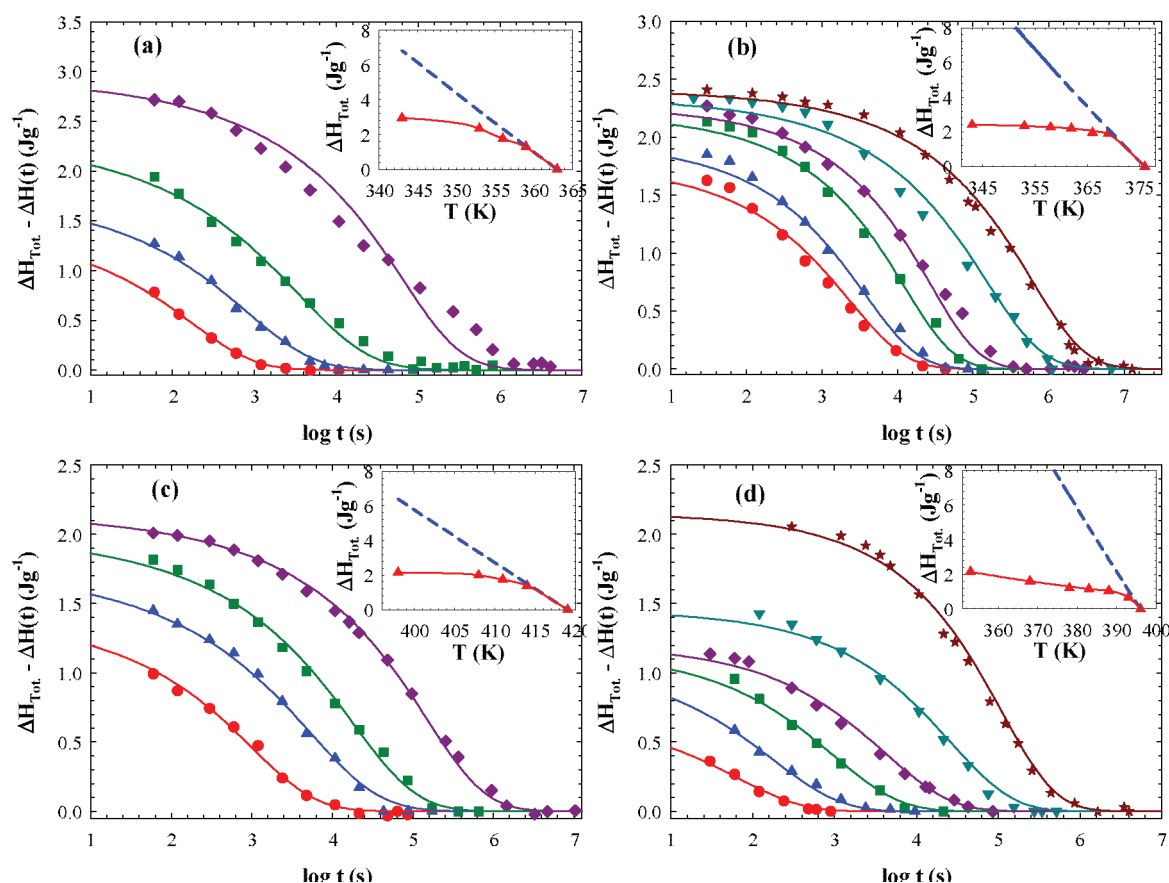


**Figure 3.** Time evolution of the recovered enthalpy at different temperatures for (a) PS7K at 359 K (red circles), 356 K (blue up-triangles), 353 K (green squares), and 343 K (violet diamonds); (b) PS85K at 369 K (red circles), 366 K (blue up-triangles), 362 K (green squares), 358 K (violet diamonds), 353 K (cyan down-triangles), and 343 K (brown stars); (c) PC at 414 K (red circles), 411 K (blue up-triangles), 408 K (green squares), and 398 K (violet diamonds); (d) PMMA at 393 K (red circles), 388 K (blue up-triangles), 383 K (green squares), 378 K (violet diamonds), 368 K (cyan down-triangles), and 353 K (brown stars). The straight lines are the fits of the data to the TNM model. The insets display the total recovered enthalpy after prolonged aging (red triangles) and the corresponding interpolation (red line) and the one that would be recovered if the melt enthalpy was extrapolated from above  $T_g$  to the aging temperature (dashed blue lines).

$T_{a1}$  followed by up-jump to  $T_{a2}$ —the system evolves until point E of Figure 1. Thus, we can conclude that, whatever the thermodynamic path imposed to the glass former, the plateau reached by the enthalpy after prolonged isothermal aging corresponds to a minimum in the energy.

## PHENOMENOLOGICAL DESCRIPTION

In the present section, we employ the Tool–Narayanaswamy–Moynihan (TNM) model<sup>51–53</sup> to describe enthalpy recovery data presented in the previous section of the paper. The main aim of this section is to show that, within the asymmetry of approach, up-jump and down-jump experiments can be described with the same set of parameters, thus demonstrating that the same molecular mechanism enables to achieve the energy minimum corresponding to the gray line in Figure 1. According to the TNM model, the spontaneous evolution of the thermodynamic state occurring during physical aging depends on both the temperature and the thermodynamic state of the glass. Such a dependence is summarized by the following two equations:

$$\Delta H_{\text{Tot}} - \Delta H(t) = \Delta H_{\text{Tot}} \exp \left\{ - \int_0^t \left( \frac{t'}{\tau} \right) dt' \right\}^{\beta_{\text{KWW}}} \quad (2)$$

and

$$\tau = A \exp \left( \frac{x \Delta h^*}{k T_a} + \frac{(1-x) \Delta h^*}{k T_f} \right) \quad (3)$$

where  $\tau$ ,  $\beta_{\text{KWW}}$ ,  $A$ ,  $x$ ,  $\Delta h^*$ , and  $T_f$  are respectively the relaxation time for physical aging, the stretching exponent, a pre-exponential factor, the nonlinearity parameter, the TNM activation energy, and the fictive temperature.

Equation 2 expresses a typical signature of the dynamics of glass-forming liquids, namely the intrinsically nonexponential behavior of any relaxation.<sup>54</sup> Equation 3 quantitatively provides a measure of the effect of the thermodynamic state on the relaxation time for physical aging, the so-called nonlinearity. This is mainly given by the nonlinearity parameter  $x$  and the fictive temperature  $T_f$ . The latter can be defined as the temperature at which a glass with a given structure would be in equilibrium<sup>51</sup> (the latter defined extrapolating the enthalpy of the melt to temperatures below  $T_g$ ). According to this definition,  $T_f$  can be written as  $T_f = T_a + ((\Delta H_{\text{Tot Extr}} - \Delta H(t))/\Delta C_p)$ , where, in this case,  $\Delta H_{\text{Tot Extr}}$  is the enthalpy that would be recovered if the thermodynamic state of the melt was extrapolated to the aging temperature and  $\Delta C_p$  is the difference between the melt and the glass specific heat.

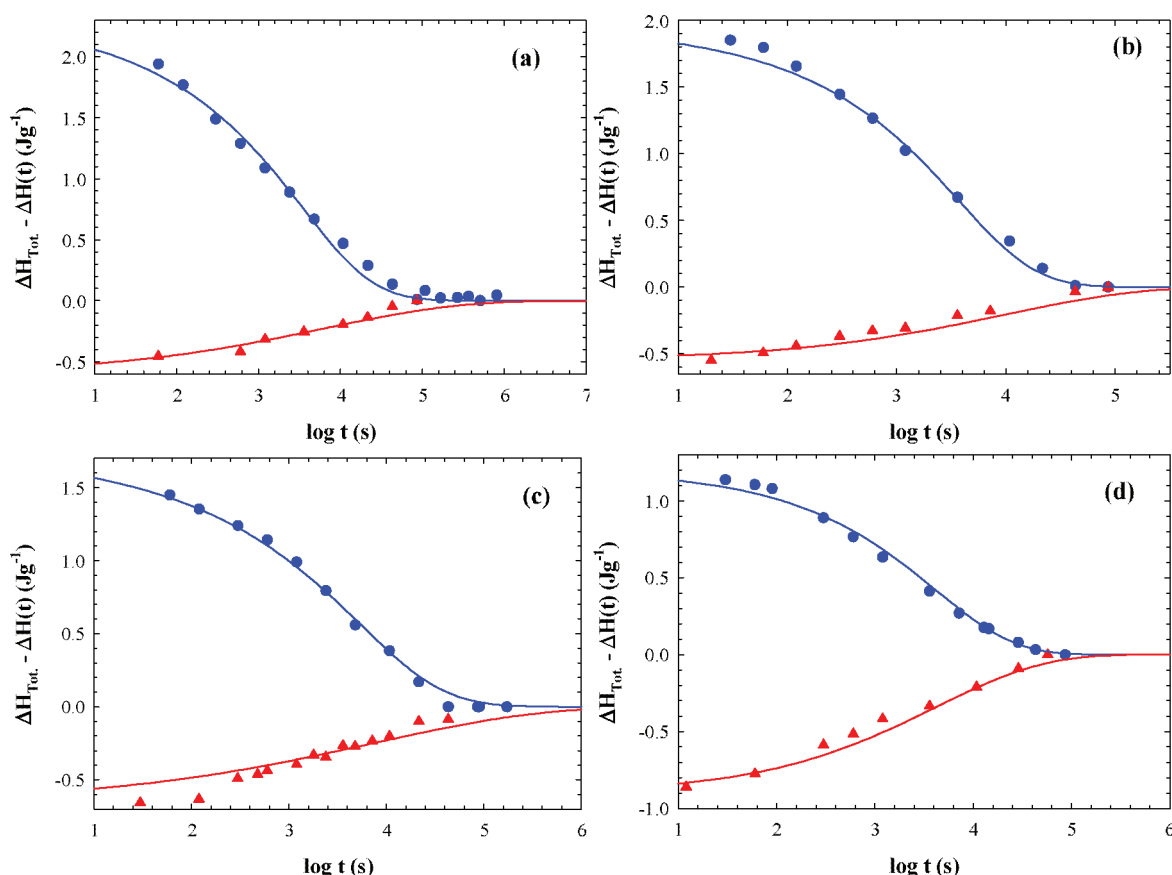


**Figure 4.** Time evolution of the recovered enthalpy after down-jump (blue circles) and up-jump (red triangles) experiments (see text for details) for (a) PS7K, (b) PS85K, (c) PC, and (d) PMMA.

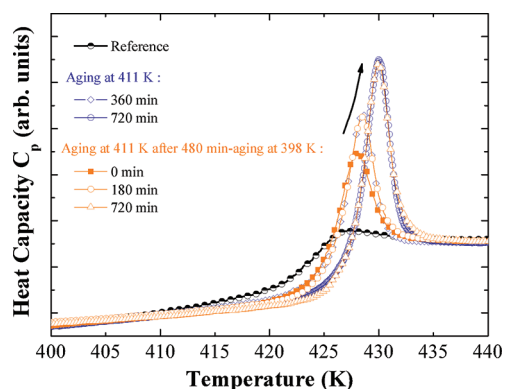


**Figure 5.** Specific heat versus temperature for PC, as a showcase, obtained by direct down-jump to  $T_{a2}$  (411 K) and by a first partial annealing at  $T_{a1}$  (398 K) followed by up-jump to  $T_{a2}$  (411 K). Details on the thermal history corresponding to the DSC scans are reported in the figure.

The TNM model can be fitted to the experimental data having  $\beta_{\text{KWW}}$ ,  $A$ , and  $\alpha$  as fitting parameters. The stretching parameter  $\beta_{\text{KWW}}$  and the nonlinearity parameter  $\alpha$  are generally found to be correlated by  $\alpha = (\beta_{\text{KWW}} - 0.2)/1.05$ .<sup>55</sup> This reduces the number of fitting parameters. Furthermore, the magnitude of the fitted value of  $A$  depends on the choice of  $\Delta h^*$ . The latter is generally given the value of the activation energy of the  $\alpha$  process in proximity of  $T_g$ .<sup>56</sup> This can be conveniently obtained from relaxation data available in the

literature.<sup>18,40–43</sup> These values are listed in Table 1 for all investigated polymers.

It is worth emphasizing that the assumption of a temperature independent activation energy  $\Delta h^*$  generally constitutes a major drawback of the TNM model. This aspect has been highlighted in details in a recent paper by Mauro et al.,<sup>57</sup> where a number of phenomenological models, included the TNM, has been tested on selenium experimental viscosity data and computed via the enthalpy landscape approach.<sup>58</sup> Such analysis clearly indicated the superior accuracy of the model proposed in that work<sup>57</sup> in comparison to others. This arises from the ability of the presented model to catch the actual temperature dependence of the equilibrium viscosity below  $T_g$ .<sup>14</sup> Despite the aforementioned limitations of the TNM model, within the scope of the present analysis—aiming to demonstrate the equivalence of the molecular mechanism involved in the achievement of equilibrium after down and up-jump experiments—we believe that this model can still be considered acceptable, overall considering the mathematical compensation of the activation energy by the factor  $A$ .

The fits of the TNM model to enthalpy recovery data of all investigated polymers are reported as continuous lines in Figures 3 and 4. The fitting parameters  $\beta_{\text{KWW}}$ ,  $A$ , and  $\alpha$  are reported in Table 1. The observation of Figures 3 and 4 suggests that the TNM model appropriately fits experimental data, included those reporting the enthalpy evolution after up-jump experiments. The stretching exponent  $\beta_{\text{KWW}}$  and the nonlinearity parameter  $\alpha$  depend on the polymer and only weakly on

temperature, being generally larger at higher temperatures. The pre-exponential factor  $A$  slightly depends on the temperature. The set of parameters relevant to fit enthalpy recovery data after a down-jump from above  $T_g$  is also able to adequately catch the enthalpy recovery after an up-jump from a lower temperature where the plateau was already reached.

## DISCUSSION

In the preceding sections of the paper, we have shown that several typical polymeric glasses subjected to a variety of thermal histories reach, after prolonged aging, a thermodynamic state significantly different from that expected from linear mere extrapolation of the thermodynamic state from above  $T_g$ . In particular, as exemplified in Figure 1, the thermodynamic state achieved by the glasses corresponds to an enthalpy consistently larger than that corresponding to the extrapolated one. Furthermore, the description of enthalpy recovery data through the TNM model suggests that the molecular mechanism responsible for the achievement of the long-term plateau is identical for all glass thermal histories, namely, simple down-jump from above  $T_g$  and up-jump to an aging temperature  $T_{a2}$  after aging at a lower temperature  $T_{a1}$ .

These results generally indicate that the thermodynamic state achieved after prolonged aging corresponds to a relative energy minimum. The main open question that needs to be formulated is whether a glass in this thermodynamic state is stable over any time scale or rather corresponds to a relative minimum with further evolution on much larger time scales. To answer this question, longer aging experiments should be performed or different densification paths be followed in an attempt of achieving a lower enthalpy state than that found after prolonged isothermal aging.

In case the obtained stable thermodynamic state after the employed annealing time is the only achievable by these polymer glasses, the most important implication is that the Kauzmann entropy crisis<sup>7</sup> would be naturally avoided as proposed by several authors.<sup>23–25,36</sup> In particular, the relatively steep temperature gradient observed in glass-forming liquids above  $T_g$  would gradually smooth at lower temperatures as indicated by the gray line in Figure 1, thus avoiding the entropy crisis. In other words, no violation of the third principle of thermodynamics would result from this scenario.

Regarding the possibility that other energy minima with lower enthalpy can be obtained, this may be the case of vapor-deposited glasses.<sup>37,38</sup> This procedure actually allows achieving low molecular mass glasses with enthalpy substantially lower than that achievable by standard isothermal aging experiments. Furthermore, the obtained structure seems to be substantially different from the one that would be obtained if the properties of the melt above  $T_g$  were extrapolated to lower temperatures.<sup>59,60</sup> Despite the unusually low enthalpy of vapor-deposited glasses, the stability of low enthalpy vapor deposited glasses has not been studied so far. Therefore, no conclusions about the long-term evolution of the so-produced glasses can be given until the direction of the enthalpy evolution of these glasses is not probed at temperatures corresponding to  $T_{a2}$  in the scheme of Figure 1.

It is worth noticing that, among the investigated polymers, that displaying the weakest deviations from the extrapolated line is PS7K (see inset of Figure 3a). In particular, the recovered enthalpy of this polymer at fixed distance from  $T_g$  is generally larger than that of the high molecular weight counterpart

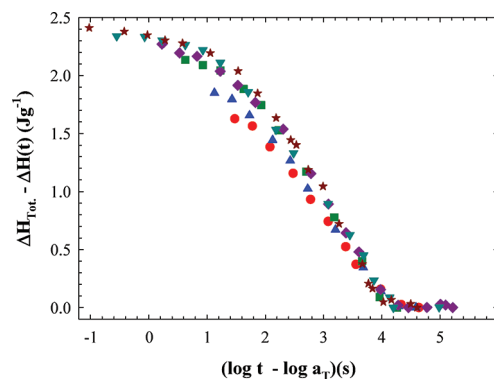


**Figure 6.** Aging time–temperature superposition of enthalpy recovery data for PS85K.

(PS85K). A similar result has been found by Andreozzi et al.<sup>31</sup> investigating the molecular weight dependence of the recovered enthalpy in PMMA. Interestingly, these authors found a cross-over in the amount of recovered enthalpy, when passing from the nonentangled to entangled regime. The results of the present study generally agree with those of Andreozzi et al.,<sup>31</sup> considering that PS7K has a molecular weight smaller than that between entanglements (about 15 000 g mol<sup>−1</sup> for PS). In the same direction as Andreozzi et al.'s results,<sup>31</sup> a recent work by Richert<sup>61</sup> on low molecular weight poly(vinyl acetate) also indicates that deviations from the behavior expected considering the melt properties are negligible below the  $T_g$ , at least in the investigated temperature range. This aspect is currently the subject of our investigation.

Another interesting aspect of the presented enthalpy recovery results regards the temperature dependence associated with the time scale needed to reach equilibrium. To obtain information on this issue, we have performed aging time–temperature superposition of enthalpy recovery curves in a way that data at long aging times (just before the plateau is achieved) collapse.<sup>17</sup> In doing so, the temperature dependence of the time scale in a nearly equilibrated state is approximately obtained, minimizing the time-dependent effects, particularly on the activation energy,<sup>17,19</sup> expected during the course of aging. The shifting procedure is displayed in Figure 6 for PS85K as a showcase. Figure 7 provides the shift factor as a function of the inverse of the temperature for all investigated polymers (solid symbols). We can compare the obtained shift factors with those obtained assuming that the  $\alpha$  relaxation—as obtained from the literature<sup>18,40–42</sup> by BDS above  $T_g$ —maintains its VFT character also below the glass transition range. This is done in Figure 7 (dashed lines), where the temperature variation of the shift factor according to the VFT law—applied in the relevant temperature range—is presented:<sup>3–5</sup>

$$a_T \sim \exp\left(\frac{B}{T - T_0}\right) \quad (4)$$

The parameter  $B$  and the Vogel temperature  $T_0$  of the VFT law fitting experimental data from BDS are<sup>18,40–42</sup>  $B = 1310$  K and  $T_0 = 318$  K for PS7K,  $B = 1325$  K and  $T_0 = 330$  K for PS85K,  $B = 1500$  K and  $T_0 = 373$  K for PC, and  $B = 1350$  K and  $T_0 = 334$  K for PMMA. As it is possible to observe in Figure 7, in all cases the shift factors at the plateau significantly deviate from those obtained extrapolating the VFT law below the glass transition range. Thus, time–temperature superposition of enthalpy recovery

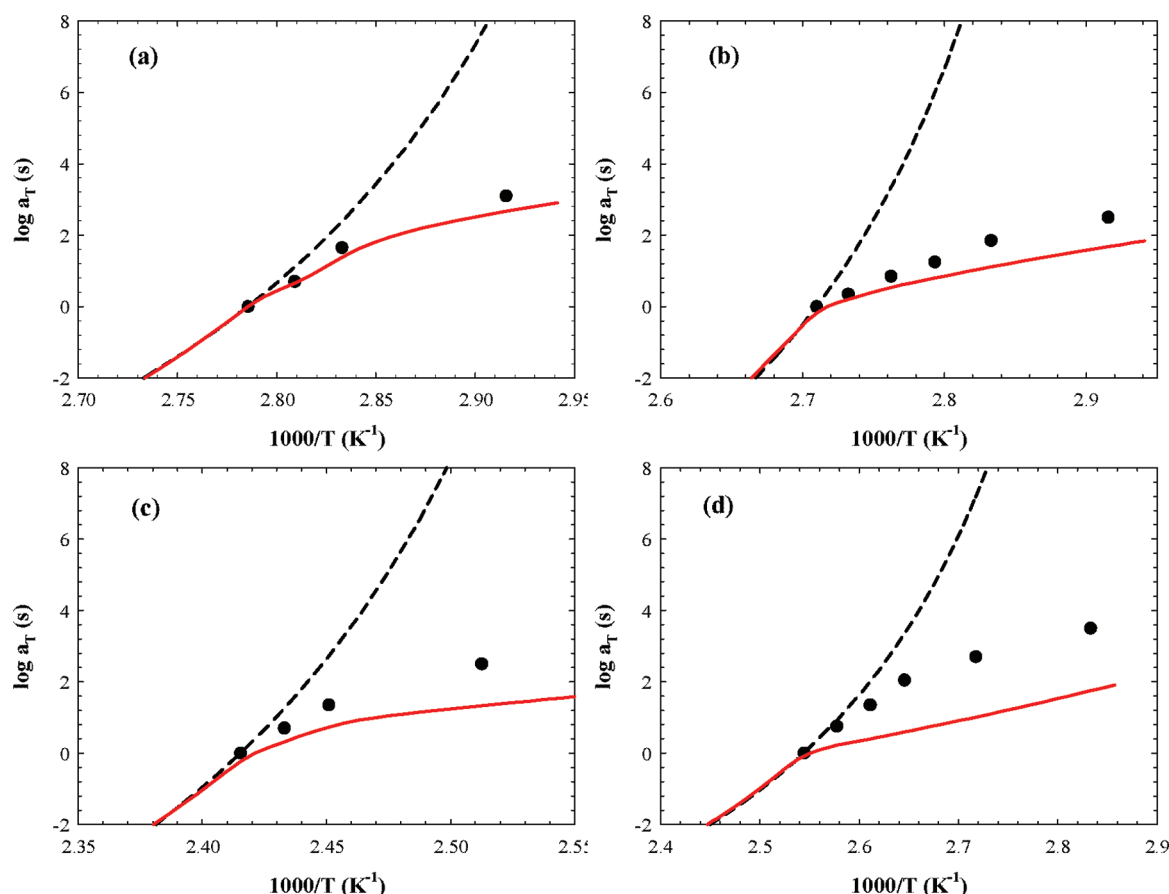


**Figure 7.** Logarithm of the shift factors as a function of the inverse temperature obtained from aging time–temperature superposition of enthalpy recovery data (symbols), derived from the temperature dependence of the  $\alpha$  relaxation according to the VFT equation (black dashed lines), and determined from the plateau values of the enthalpy employing the AG equation (continuous red lines). (a) PS7K, (b) PS85K, (c) PC, and (d) PMMA.

data close to the plateau (see Figure 6) delivers activation energies systematically smaller than those associated with the  $\alpha$  process described by the VFT law. This implies that either the  $\alpha$  process undergoes a dramatic crossover in its temperature dependence<sup>4,16,17</sup> or secondary relaxation processes play a major role in the equilibration of the glass.<sup>18,19,21,62,63</sup> In the former case, it is interesting to notice that the deviation of the  $\alpha$  process from the VFT behavior predicted by Mauro and co-workers<sup>14,57</sup> is, at least qualitatively, compatible with that found by us applying the aging time–temperature superposition to our enthalpy data as explained.

So far the present discussion has highlighted the deviation from the behavior expected by mere extrapolation of equilibrium data from above  $T_g$  of both thermodynamics and dynamics. Considering that a relevant line of thought in the description of glass-forming liquids is that thermodynamics and dynamics are intimately connected, it is natural to investigate whether this framework is also able to catch the phenomenology encountered in this work below the glass transition range. To do so, we have employed the AG theory<sup>39</sup> of the glass transition connecting the relaxation time of the  $\alpha$  relaxation to the configurational entropy  $S_c$ , which in terms of shift factor reads

$$a_T \sim \exp\left(\frac{C}{TS_c}\right) \quad (5)$$

where  $C$  is a material specific and temperature independent parameter. The configurational entropy is experimentally

inaccessible but as it has been shown<sup>64</sup> the AG still remains suitable when  $S_c$  is replaced by the excess entropy related to the  $\alpha$  process  $S_{ex-\alpha}$ , namely the difference between the entropy of the melt associated with the  $\alpha$  process and that of the corresponding crystal. The latter can be evaluated as  $S_{ex-\alpha}(T) = \int_{T_0}^T (\Delta C_p/T) dT$ , where  $\Delta C_p$ , the excess specific heat, is the difference between the melt and the crystal specific heats—the latter approximated to that of the glass—respectively  $C_{p-mel}$  and  $C_{p-gl}$ . The latter can be promptly obtained from the literature.<sup>44,45</sup>  $C_{p-mel}$  above  $T_g$  is also reported in refs 44 and 45 for the investigated polymers, whereas that below  $T_g$  is obtained interpolating and deriving the enthalpy corresponding to the plateau (reported in Table 1 and the insets of Figure 3). Fitting literature data<sup>18,40–42</sup> delivers the following values for this parameter:  $C = 535 \text{ J g}^{-1}$  for PS7K,  $C = 505 \text{ J g}^{-1}$  for PS85K,  $C = 425 \text{ J g}^{-1}$  for PC, and  $C = 565 \text{ J g}^{-1}$  for PMMA.

For evaluating  $S_{ex-\alpha}$  in the relevant temperature range here, the measured values of the total enthalpy change—reported in Table 1 and depicted in the insets of Figure 3—has been used to obtain interpolating lines (see solid red lines in these insets) accounting also for the equilibrium behavior above  $T_g$ . The shift factors as evaluated from the AG equation are shown as red lines in Figure 7. As can be observed, although the AG prediction tends to underestimate the shift factors obtained by aging time–temperature superposition of enthalpy recovery data, it captures rather well the general trend, the worse case being PMMA. In this particular polymer, it is well-known that a very prominent



secondary relaxation is detected close to  $T_g$  (it is the dominant dielectric relaxation).<sup>65</sup> Taking this into account, one could speculate that the secondary relaxation in PMMA has a more relevant role in the equilibration process than in the other polymers. In fact, by simple inspection of Figure 2, it is obvious that the enthalpy relaxation features in the DSC trace are qualitatively different in this polymer. Thus, the consistency of the AG prediction with shift factors data can generally be considered reasonable. This result suggests that the thermodynamic approach to the description of the dynamics of glass formers may be applied also below the glass transition range.

## CONCLUSIONS

We have performed a systematic study on the enthalpy recovery of several glass-forming polymers during long-term aging. We generally find that, independently of the followed thermodynamic path, the achieved thermodynamic state is the same at each temperature and considerably deviates from that expected by extrapolating thermodynamic properties from above  $T_g$ . In particular, the stability of such thermodynamic state is indicated by monitoring the evolution of the enthalpy after (i) simple down-jump experiments from above  $T_g$ , (ii) up-jump experiments at  $T_{a2}$  after achievement of equilibrium at  $T_{a1}$ , and (iii) up-jump experiments at  $T_{a2}$  after partial aging at  $T_{a1}$ .

The obtained results suggest that an energy minimum far different from that corresponding to that of the extrapolated melt is achieved. This minimum could either be the only achievable by systems deep in the glassy state or just a relative one. The former scenario is discussed in relation to the possible solution of the Kauzmann paradox, since the considerably milder temperature dependence of thermodynamic variables in comparison to the extrapolated one would prevent the entropy of the glass from becoming smaller than the one of the crystal. The possible presence of other energy minima is discussed considering other thermodynamic routes able to generate enthalpy states considerably lower than that achieved after classical aging.

Finally, through an aging time—temperature superposition of the long-term enthalpy recovery data, it has been shown that the molecular mechanism responsible for the equilibration of the glass substantially deviates from the VFT behavior normally valid above  $T_g$ . The possible connection between this deviation and that of thermodynamics has been scrutinized applying the AG theory. The results suggest that such connection is, at least qualitatively, realistic.

## AUTHOR INFORMATION

### Corresponding Author

\*E-mail: swxcacad@sw.ehu.es.

## ACKNOWLEDGMENT

The authors acknowledge the University of the Basque Country and Basque Country Government (Ref. No. IT-436-07, Depto. Educación, Universidades e Investigación) and Spanish Minister of Education (Grant No. MAT 2007-63681 and CSD2006-00053) for their support. The support of the Basque Government within the Etorrek program is also acknowledged.

## REFERENCES

(1) Debenedetti, P. G. *Metastable Liquids: Concepts and Principles*; Princeton University Press: Princeton, 1996.

- (2) Struik, L. *Physical Aging in Amorphous Materials and Other Materials*; Elsevier: Amsterdam, 1978.
- (3) Vogel, H. *Phys. Z.* **1921**, 22, 645–646.
- (4) Fulcher, G. S. *J. Am. Ceram. Soc.* **1925**, 8, 339–355.
- (5) Tammann, G.; Hesse, W. *Z. Anorg. Allg. Chem.* **1926**, 156, 245.
- (6) Williams, M.; Landel, R.; Ferry, J. D. *J. Am. Chem. Soc.* **1955**, 77, 3701–3707.
- (7) Kauzmann, W. *Chem. Rev.* **1948**, 43, 219–256.
- (8) Cangialosi, D.; Alegria, A.; Colmenero, J. *Europhys. Lett.* **2005**, 70, 614–620.
- (9) Cangialosi, D.; Alegria, A.; Colmenero, J. *J. Chem. Phys.* **2006**, 124, 024906.
- (10) Angell, C. A. *J. Res. Natl. Inst. Stand. Technol.* **1997**, 102, 171–185.
- (11) Avramov, I.; Milchev, A. *J. Non-Cryst. Solids* **1988**, 104, 253–260.
- (12) Kivelson, D.; Kivelson, S.; Zhao, X.; Nussinov, Z.; Tarjus, G. *Physica A* **1995**, 219, 27–38.
- (13) Di Marzio, E.; Yang, A. *J. Res. Natl. Inst. Stand. Technol.* **1997**, 102, 135–157.
- (14) Mauro, J. C.; Yue, Y.; Ellison, A. J.; Gupta, P. K.; Allan, D. C. *Proc. Natl. Acad. Sci. U. S. A.* **2009**, 106, 19780–19784.
- (15) Elmatad, Y. S.; Chandler, D.; Garrahan, J. P. *J. Phys. Chem. B* **2009**, 113, 5563–5567.
- (16) O'Connell, P.; McKenna, G. J. *Chem. Phys.* **1999**, 110, 11054–11060.
- (17) Simon, S.; Sobieski, J.; Plazek, D. *Polymer* **2001**, 42, 2555–2567.
- (18) Cangialosi, D.; Wubbenhorst, M.; Schut, H.; van Veen, A.; Picken, S. *Phys. Rev. B* **2004**, 69, 134206.
- (19) Chen, K.; Vyazovkin, S. *J. Phys. Chem. B* **2009**, 113, 4631–4635.
- (20) Hecksher, T.; Nielsen, A. I.; Olsen, N. B.; Dyre, J. C. *Nature Phys.* **2008**, 4, 737–741.
- (21) Mao, C.; Chamarthy, S. P.; Byrn, S. R.; Pinal, R. *J. Phys. Chem. B* **2010**, 114, 269–279.
- (22) Dimopoulos, A.; Wietor, J.-L.; Wubbenhorst, M.; Napolitano, S.; van Benthem, R. A. T. M.; de With, G.; Sijbesma, R. P. *Macromolecules* **2010**, 43, 8664–8669.
- (23) Stillinger, F. H. *J. Chem. Phys.* **1988**, 88, 7818–7825.
- (24) Pyda, M.; Wunderlich, B. *J. Polym. Sci., Part B: Polym. Phys.* **2002**, 40, 1245–1253.
- (25) Wolfgardt, M.; Baschnagel, J.; Paul, W.; Binder, K. *Phys. Rev. E* **1996**, 54, 1535–1543.
- (26) Yan, Q.; Jain, T.; de Pablo, J. *Phys. Rev. Lett.* **2004**, 92, 235701.
- (27) Ottinger, H. C. *Phys. Rev. E* **2006**, 74, 011113.
- (28) Cowie, J.; Harris, S.; McEwen, I. J. *Polym. Sci., Part B: Polym. Phys.* **1997**, 35, 1107–1116.
- (29) Brunacci, A.; Cowie, J. M. G.; Ferguson, R.; McEwen, I. J. *Polymer* **1997**, 38, 3263–3268.
- (30) Duenas, J.; Garayo, A.; Colomer, F.; Estelles, J.; Ribelles, J.; Pradas, M. *J. Polym. Sci., Part B: Polym. Phys.* **1997**, 35, 2201–2217.
- (31) Andreozzi, L.; Faetti, M.; Giordano, M.; Zulli, F. *Macromolecules* **2005**, 38, 6056–6067.
- (32) Boucher, V. M.; Cangialosi, D.; Alegria, A.; Colmenero, J. *Macromolecules* **2010**, 43, 7594–7603.
- (33) Boucher, V. M.; Cangialosi, D.; Alegria, A.; Colmenero, J.; Pastoriza-Santos, I.; Liz-Marzan, L. M. *Soft Matter* **2011**, 7, 3607–3620.
- (34) Li, Q.; Simon, S. L. *Polymer* **2006**, 47, 4781–4788.
- (35) Rault, J. *Physical Aging of Glasses*; Nova Science Publisher Inc.: New York, 2009.
- (36) Johari, G. P. *J. Chem. Phys.* **2000**, 113, 751–761.
- (37) Swallen, S. F.; Kearns, K. L.; Mapes, M. K.; Kim, Y. S.; McMahon, R. J.; Ediger, M. D.; Wu, T.; Yu, L.; Satija, S. *Science* **2007**, 315, 353–356.
- (38) Leon-Gutierrez, E.; Garcia, G.; Clavaguera-Mora, M. T.; Rodriguez-Viejo, J. *Thermochim. Acta* **2009**, 492, 51–54.
- (39) Adam, G.; Gibbs, J. J. *J. Chem. Phys.* **1965**, 43, 139.
- (40) Boucher, V. M.; Cangialosi, D.; Alegria, A.; Colmenero, J., unpublished results.

- (41) Hintermeyer, J.; Herrmann, A.; Kahlau, R.; Goiceanu, C.; Roessler, E. A. *Macromolecules* **2008**, *41*, 9335–9344.
- (42) van den Berg, O.; Sengers, W.; Jager, W.; Picken, S.; Wubbenhorst, M. *Macromolecules* **2004**, *37*, 2460–2470.
- (43) Theobald, S.; Pechhold, W.; Stoll, B. *Polymer* **2001**, *42*, 289–295.
- (44) Wunderlich, B.; Pyda, M. <http://athas.prz.edu.pl/>, 2005–2011.
- (45) Wunderlich, B. *Thermal Analysis of Polymeric Materials*; Springer-Verlag: Berlin, 2005.
- (46) Kovacs, A. J. *Fortschr. Hochpolym.-Forsch.* **1963**, *3*, 394–507.
- (47) Hodge, I. J. *Non-Cryst. Solids* **1994**, *169*, 211–266.
- (48) Borde, B.; Bizot, H.; Vigier, G.; Buleon, A. *Carbohydr. Polym.* **2002**, *48*, 111–123.
- (49) Alves, N.; Ribelles, J.; Mano, J. *Polymer* **2005**, *46*, 491–504.
- (50) Hodge, I. *Macromolecules* **1987**, *20*, 2897–2908.
- (51) Tool, A. J. *Am. Ceram. Soc.* **1946**, *29*, 240–253.
- (52) Narayanaswamy, O. J. *Am. Ceram. Soc.* **1971**, *54*, 491–498.
- (53) Moynihan, C.; Macedo, P.; Montrose, C.; Gupta, P.; De Bolt, M.; Dill, J.; Dom, B.; Drake, P.; Easteal, A.; Elterman, P.; Moeller, R.; Sasabe, H.; Wilder, J. *Ann. N.Y. Acad. Sci.* **1976**, *279*, 15–35.
- (54) Williams, G.; Watts, D. *Trans. Faraday Soc* **1970**, *66*, 80–85.
- (55) Hodge, I. J. *Res. Natl. Inst. Stand. Technol.* **1997**, *102*, 195–205.
- (56) Hodge, I.; Berens, A. *Macromolecules* **1982**, *15*, 762–770.
- (57) Mauro, J. C.; Allan, D. C.; Potuzak, M. *Phys. Rev. B* **2009**, *80*, 094204.
- (58) Mauro, J. C.; Loucks, R. J.; Gupta, P. K. *J. Phys. Chem. A* **2007**, *111*, 7957–7965.
- (59) Dawson, K. J.; Kearns, K. L.; Yu, L.; Steffen, W.; Ediger, M. D. *Proc. Natl. Acad. Sci. U. S. A.* **2009**, *106*, 15165–15170.
- (60) Souda, R. *J. Phys. Chem. B* **2010**, *114*, 11127–11132.
- (61) Richert, R. *Physica A* **2000**, *287*, 26–36.
- (62) Nemilov, S.; Johari, G. *Philos. Mag.* **2003**, *83*, 3117–3132.
- (63) Hu, L.; Yue, Y. *J. Phys. Chem. B* **2008**, *112*, 9053–9057.
- (64) Angell, C.; Borick, S. J. *Non-Cryst. Solids* **2002**, *307*, 393–406.
- (65) Bergman, R.; Alvarez, F.; Alegria, A.; Colmenero, J. *J. Chem. Phys.* **1998**, *109*, 7546–7555.